

# Tunable Surface-Normal Modulators Operating Near 1550 nm With a High-Extinction Ratio at High Temperatures

H. Mohseni, W. K. Chan, H. An, A. Ulmer, and D. Capewell

**Abstract**—We present high-performance surface-normal modulators based on unique properties of stepped quantum wells at an eye-safe wavelength of 1550 nm. Fabricated devices show higher efficiency and a 7-dB higher extinction ratio compared with devices with coupled quantum-well active layers. Moreover, the energy band edge of the device can be tuned over 70 nm while maintaining a 3-dB modulation depth. Such a wide tuning range eliminates the need for a thermoelectric cooler and is a critical advantage for many applications such as unmanned aerial vehicles and dynamic optical tags. The devices show good performance up to the maximum measured temperature of 70 °C.

**Index Terms**—Modulator, optical tag, quantum well, surface-normal, stepped quantum well, tunable modulator.

## I. INTRODUCTION

**S**URFACE-NORMAL optical modulators are attractive devices for a wide range of applications such as free-space photonic links for mobile platforms [1], chip-to-chip optical interconnects [2], high-speed transceivers [3], optical correlators [4], and optical vector-matrix multipliers [5]. Surface-normal modulators based on multi-quantum wells are the prime candidates for applications with frequencies above hundreds of kilohertz. Unfortunately, this technology suffers from a small optical bandwidth, since the operating wavelength must be very close to the semiconductor optical absorption edge. Narrow optical bandwidth is particularly unfavorable, since a small change of modulator temperature can change the modulator bandgap and hence reduce the modulation depth significantly. This process necessitates a closed-loop temperature controller and leads to significantly higher system power consumption, cost, volume, and weight.

Other important parameters of a surface-normal modulator are the modulator power consumption and data bandwidth. Reducing the device area can improve the power consumption and data bandwidth, since the former is directly and the latter is inversely proportional to the device capacitance. Unfortunately, reducing the device area can significantly degrade the link performance. For example, the gain of a photonic link based on a retroreflector is proportional to the fourth power of the modulator area [1]. Recently, coupled quantum wells have been used

to reducing the operating voltage, and hence the power consumption, of the modulators [6]. However, the data bandwidth of these devices is still limited by high device capacitance, and the optical bandwidth is only 10 nm. Another method to reduce the operating voltage is to use asymmetric Fabry–Pérot modulators [5]. Unfortunately, this method reduces the field of view and optical bandwidth significantly. Here, we report on realization of a tunable large area surface-normal modulator based on novel stepped quantum wells (SQWs) [7], [8] with a significantly smaller reduction of the optical absorption at high-electric fields compared with conventional quantum wells. These devices show very low capacitance per unit area, wide field of view, high-extinction ratio, high efficiency, high tunability, and high-operating temperature.

## II. DEVICE FABRICATION

Modulator structure is based on GaInAsP–AlInAs material grown by low-pressure metal–organic vapor phase epitaxy (MOVPE) on n-type InP substrates. The active layer contains 248 periods of SQWs with a total thickness of about 5  $\mu\text{m}$  and is sandwiched between the n-doped InP and a 1- $\mu\text{m}$ -thick p-doped AlInAs layer. The nominal composition and thickness of the layers in each period are  $\text{In}_{0.54}\text{Ga}_{0.46}\text{As}$  (50 Å),  $\text{In}_{0.59}\text{Ga}_{0.41}\text{As}_{0.89}\text{P}_{0.11}$  (29 Å),  $\text{In}_{0.70}\text{Ga}_{0.30}\text{As}_{0.64}\text{P}_{0.36}$  (36 Å), and  $\text{In}_{0.53}\text{Al}_{0.47}\text{As}$  (90 Å). The measured n-type background doping level is about  $1 \times 10^{15} \text{ cm}^{-3}$ . The material is processed into modulators with different diameters from 250  $\mu\text{m}$  to 6.3 mm on 2-in InP wafers (see the inset of Fig. 1.) The device is passivated with a thin layer of silicon nitride using a conventional plasma-enhanced chemical vapor deposition (PECVD) technique.

## III. MEASUREMENT RESULTS AND DISCUSSION

High leakage current and premature breakdown are the most important sources of low yield for large area modulators. Although a reasonable extinction ratio can be obtained with our devices at about 10 V, a high reverse bias voltage is needed to obtain wide wavelength tuning range. Fig. 1 shows excellent current–voltage characteristics of a modulator with 5.1-mm diameter at zero illumination. The dark current of the device is  $\sim 10 \mu\text{A}$  at  $-95 \text{ V}$ , which is equal to a current density of  $\sim 50 \mu\text{A}/\text{cm}^2$  at an electric field of  $\sim 190 \text{ kV}/\text{cm}$ . This is similar to the lowest leakage current density of modulators based on InGaAs multi-quantum wells with a much wider bandgap

Manuscript received July 8, 2005; revised October 12, 2005.

H. Mohseni is with the Department of Electrical and Computer Engineering, Northwestern University, Evanston, IL 60208 USA (e-mail: hmohseni@ece.northwestern.edu).

W. K. Chan, H. An, A. Ulmer, and D. Capewell are with the Sarnoff Corporation, Princeton, NJ 08543 USA.

Digital Object Identifier 10.1109/LPT.2005.861629

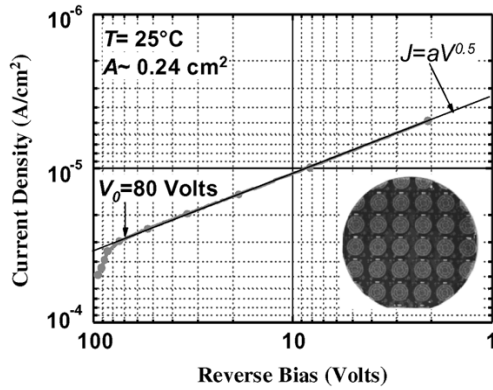


Fig. 1. Current–voltage characteristic of 5.1-mm diameter modulator without illumination. Inset shows fully processed 2-in wafer.

and at a similar electric field [9]. The device shows a generation-recombination limited dark current up to  $-80$  V. The current rapidly increases for bias voltages beyond  $-100$  V and the punched-through voltage is about  $-110$  V.

For a p-i-n structure, the punched-through voltage  $V_p$  can be calculated from [10]:  $V_p = V_B(W/W_m)(2 - W/W_m)$ , where  $V_B$  is the breakdown voltage,  $W$  is the thickness of the undoped  $i$  layer, and  $W_m$  is the depletion thickness at breakdown voltage. The universal expression for breakdown voltage in a semiconductor  $P^+ - i$  junction is [10]  $V_B = -60(E_g/1.1)^{3/2}(N_B/10^{16})^{-3/4}$ , where  $E_g$  is the material bandgap in electronvolts and  $N_B$  is the background doping level of the  $n$ -doped layer in  $\text{cm}^{-3}$ . This expression shows good agreement with experimental data for the breakdown voltages of bulk InP, with a bandgap of 1.344 eV and bulk  $\text{Ga}_{0.47}\text{In}_{0.53}\text{As}$ , with a bandgap of 0.75 eV [11]. Also, it shows good agreement with the measured breakdown voltage of AlGaAs–GaAs multiquantum-well modulators [12] with a bandgap of  $\sim 1.47$  eV. Using the measured background doping level of  $N_B = 1 \times 10^{15} \text{ cm}^{-3}$ , an effective bandgap of  $E_g = 0.88$  eV (calculated from the quantum well's peak photoluminescence wavelength) and undoped layer thickness of  $W = 5 \mu\text{m}$ , the calculated punched-through voltage for our device is about  $-112$  V.

The optical transmission spectrum of the device is measured using a tunable laser diode and a large area photodiode. The laser beam was expanded to about 4 mm in diameter and passed through the device. The thickness of the silicon–nitride passivation layer is designed such that the layer performed as an antireflection (AR) coating. This reduces the magnitude of the Fabry–Pérot peaks to below 0.1 dB. The double-pass insertion loss is less than 1 dB for wavelengths far from the absorption edge and increases exponentially as the wavelength approaches the absorption edge. The double-pass insertion loss is about 3 dB for a  $\sim 25$ -nm detuning from the absorption peak. The double-pass extinction ratio of the device was calculated based on the measured transmission data. Fig. 2 shows the double-pass extinction ratio of a 5.1-mm device at different bias values at room temperature. The extinction is about 3.4 dB for 10 V, which is similar to the extinction ratio of coupled-quantum-well devices at 6 V [13]. However, the depleted layer of this device is more than three times thicker, and hence the capacitance per

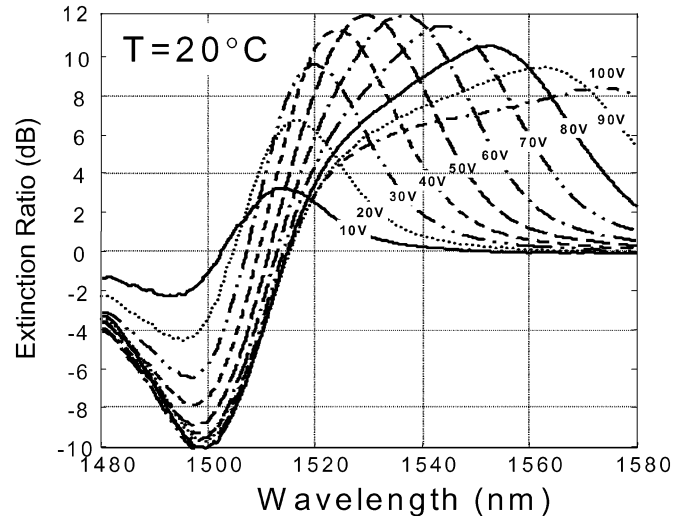


Fig. 2. Double-pass extinction ratio spectra versus applied bias for 5.1-mm modulator.

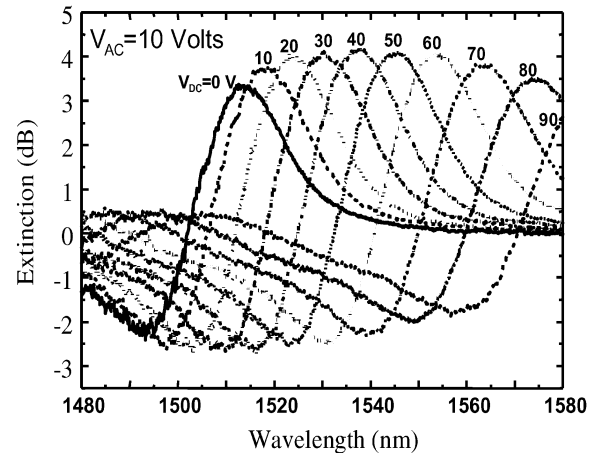


Fig. 3. Measured double-pass extinction ratio spectra for signal level of 10 V and dc bias voltages 0–90 V.

unit area is much smaller than the device with coupled quantum wells. Since power consumption of a modulator at high frequencies is proportional to  $CV^2$ , where  $C$  is the device capacitance and  $V$  is the applied voltage, the current device consumes nearly 20% lower power. The maximum extinction ratio of the modulator exceeds 12 dB, which is important for analog applications. The absence of an internal cavity in this device provides an extremely wide field of view exceeding  $\pm 60^\circ$  of the surface-normal axis, which is crucial for mobile platform applications. The device capacitance is about 0.5 nF.

In contrast to analog applications, digital applications do not require a high-extinction ratio. In fact, one can show that in a free-space optical link based on retromodulators, an extinction ratio of 3 dB produces a signal-to-noise ratio that is about 89% of the maximum possible value [14]. Fig. 3 shows the extinction ratio of the modulator versus wavelength by applying a signal level of 10 V (peak to peak) in addition to a tuning dc voltage from 0–90 V. The modulator shows a dc tuning range of more than 70 nm for an extinction ratio above 3 dB. The measured change of absorption edge versus temperature for this device

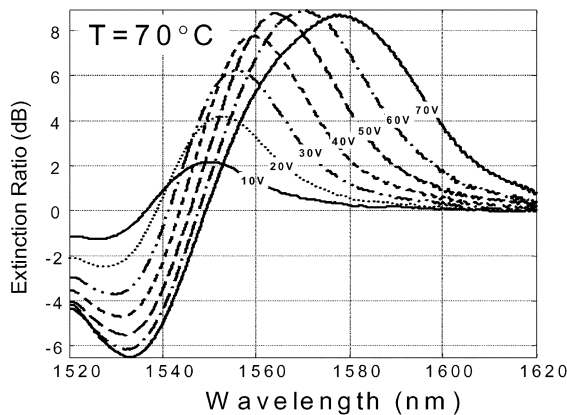


Fig. 4. Double-pass extinction ratio spectra versus applied bias for 5.1-mm modulator at 70 °C.

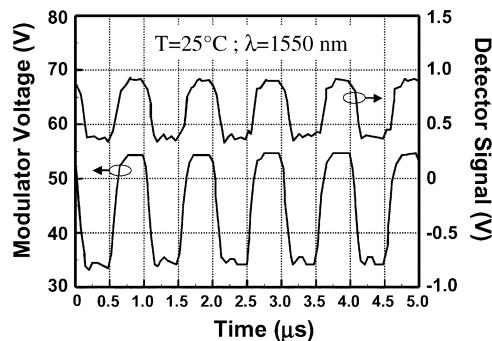


Fig. 5. Single-pass modulated optical signal (upper trace) for 1-MHz square wave input signal (lower trace.)

is about 0.7 nm/°C, which combined with the tuning range of 70 nm provides an operating temperature range of about 100 °C. Unfortunately, the performance of electroabsorption (EA) modulators can severely degrade at high temperatures. However, recent studies [15], [16] have shown that EA modulators with InAlAs barriers have a clear advantage compared with the modulators using InP barriers in this regard. Fig. 4 shows the extinction ratio spectra of our modulator at the maximum military temperature of 70 °C. Although the extinction ratio is reduced by nearly 30%, a 3-dB extinction ratio can be obtained with about 15 V. The device shows a similar insertion loss at 70 °C compared to room temperature. The dark current was about 50  $\mu$ A at 70 V at 70 °C. However, a higher dark current at higher temperatures is less significant, since the required tuning dc voltage is decreasing at higher temperatures. For instance, in order to operate near 1550 nm, the device requires  $\sim$ 55 V at 20 °C,  $\sim$ 35 V at 40 °C, and  $\sim$ 5 V at 70 °C.

The frequency response of the device was measured using a high-voltage amplifier and a fast infrared detector. Fig. 5 shows the modulated optical signal (single-pass) for a 20-V peak-to-peak square wave input signal at 1 MHz at  $\lambda \sim$ 1550 nm. The large-signal performance is limited by the maximum output current of the driver to about 200 ns rise and fall times. However, the small-signal 3-dB frequency bandwidth of the device exceeds 10 MHz.

#### IV. CONCLUSION

Large-area surface-normal modulators based on novel SQWs are demonstrated. The devices show more than 12-dB extinction ratio and nearly 70-nm tunable range, while they consume a lower power compared with the best coupled quantum-well devices with a similar extinction ratio. More importantly, these devices can compensate thermal band edge shift over 100 °C applying about 90 V, which combined with a low leakage current of about 10  $\mu$ A result in a maximum of  $\sim$  900  $\mu$ W of dc power. This is about two orders of magnitude less than the power required by the best TE coolers to keep the temperature of the device stable over this range.

#### REFERENCES

- [1] G. C. Gilbreath *et al.*, "Large aperture multiple quantum well modulating retroreflector for free space optical data transfer on unmanned aerial vehicles," *Opt. Eng.*, vol. 40, pp. 1348–1356, 2001.
- [2] H. Liu, C. C. Lin, and J. S. Harris, "High-speed, dual-function vertical cavity multiple quantum well modulators and photodetectors for optical interconnects," *Opt. Eng.*, vol. 40, pp. 1186–1191, 2001.
- [3] D. Yap, K. R. Elliott, Y. K. Brown, A. R. Kost, and E. S. Ponti, "High-speed integrated optoelectronic modulation circuit," *IEEE Photon. Technol. Lett.*, vol. 13, no. 2, pp. 626–628, Feb. 2001.
- [4] J. C. Kirsch, B. K. Jones, and K. Kang, "Design and evaluation of a multiple quantum well SLM based optical correlator," in *Optical Pattern Recognition XI, Proc. SPIE*, D. P. Casasent and T.-H. Chao, Eds., 2000, vol. 4043, pp. 66–71.
- [5] U. Arad, E. Redmard, M. Shamay, A. Averboukh, S. Levit, and U. Efron, "Development of a large high-performance 2-D array of GaAs-AlGaAs multiple quantum-well modulators," *IEEE Photon. Technol. Lett.*, vol. 15, no. 10, pp. 1531–1533, Oct. 2003.
- [6] T. H. Stievater, W. S. Rabinovich, P. G. Goetz, R. Mahon, and S. C. Binari, "A surface-normal coupled-quantum-well modulator at 1.55 microns," in *Proc. IEEE Conf. Lasers Electro-optics CLEO CThH3*, San Francisco, CA, May 2004.
- [7] H. Mohseni, H. An, Z. Shellenbarger, M. Kwakernaak, and J. H. Abeles, "Enhanced electro-optic effect in GaInAsP-InP three-step quantum wells," *Appl. Phys. Lett.*, vol. 84, pp. 1823–1825, 2004.
- [8] —, "Highly linear and efficient phase modulators based on GaInAsP-InP three-step quantum wells," *Appl. Phys. Lett.*, vol. 86, p. 031 103, 2005.
- [9] K. Ikossi, W. S. Rabinovich, D. S. Katzer, S. C. Binari, J. Mittereder, and P. G. Goetz, "Multiple quantum well PIN optoelectronic devices and a method of restoring failed device characteristics," *Microelectron. Reliability*, vol. 42, pp. 1021–1028, 2002.
- [10] S. Sze, *Physics of Semiconductor Devices*. New York: Wiley, 1981, pp. 104–105.
- [11] N. Arnold, R. Schmitt, and K. Heime, "Diffusion in III-V semiconductors from spin-on film sources," *J. Phys. D*, vol. 17, no. 3, pp. 443–474, 1984.
- [12] Q. Wang, S. Junique, D. Ågren, B. Noharet, and J. Y. Andersson, "Fabry-Pérot electroabsorption modulators for high-speed free-space optical communication," *IEEE Photon. Technol. Lett.*, vol. 16, no. 9, pp. 1471–1473, Sep. 2004.
- [13] T. H. Stievater, W. S. Rabinovich, P. G. Goetz, R. Mahon, and S. C. Binari, "A surface-normal coupled-quantum-well modulator at 1.55  $\mu$ m," *IEEE Photon. Technol. Lett.*, vol. 16, no. 9, pp. 2036–2038, Sep. 2004.
- [14] S. Griggs, M. Mark, and B. Feldman, "Dynamic optical tags," in *Battlespace Digitization and Network-Centric Systems IV, Proc. SPIE*, R. Suresh, Ed., 2004, vol. 5441, pp. 151–160.
- [15] N. C. Frateschi, J. Zhang, W. J. Choi, H. Gebretsadiq, R. Jambunathan, and A. E. Bond, "High performance uncooled C-band, 10 Gbit/s InGaAlAs MQW electroabsorption modulator integrated to semiconductor amplifier in laser-integrated modules," *Electron. Lett.*, vol. 40, pp. 140–141, 2004.
- [16] E. Foti, L. Fratta, F. Ghiglieno, C. Coriasso, C. Cacciatore, C. Rigo, M. Agresti, M. Vallone, S. Codato, G. Fornuto, R. Fang, M. Rosso, A. Buccieri, and P. Valenti, "Optimization of 10 Gbit/s InGaAsP electroabsorption modulator operating at high temperature," in *IEE Proc.-Optoelectron.*, vol. 151, 2004, pp. 103–108.